Available online at www.sciencedirect.com
ScienceDirect
Biochemical and Biophysical Research Communications 369 (2008) 124–134
BBRC
www.elsevier.com/locate/ybbrc

The B2 alternatively spliced isoform of nonmuscle myosin II-B lacks actin-activated MgATPase activity and *in vitro* motility

Kye-Young Kim [a], Sachiyo Kawamoto [a], Jianjun Bao [b], James R. Sellers [c], Robert S. Adelstein [a,*]

[a] *Laboratory of Molecular Cardiology, National Heart, Lung, and Blood Institute, National Institutes of Health Bethesda, MD 20892, USA*
[b] *Cardiology Branch, National Heart, Lung, and Blood Institute, National Institutes of Health Bethesda, MD 20892, USA*
[c] *Laboratory of Molecular Physiology, National Heart, Lung, and Blood Institute, National Institutes of Health Bethesda, MD 20892, USA*

Received 31 October 2007
Available online 3 December 2007

Abstract

We report the initial biochemical characterization of an alternatively spliced isoform of nonmuscle heavy meromyosin (HMM) II-B2 and compare it with HMM II-B0, the nonspliced isoform. HMM II-B2 is the HMM derivative of an alternatively spliced isoform of endogenous nonmuscle myosin (NM) II-B, which has 21-amino acids inserted into loop 2, near the actin-binding region. NM II-B2 is expressed in the Purkinje cells of the cerebellum as well as in other neuronal cells [X. Ma, S. Kawamoto, J. Uribe, R.S. Adelstein, Function of the neuron-specific alternatively spliced isoforms of nonmuscle myosin II-B during mouse brain development, Mol. Biol. Cell 15 (2006) 2138–2149]. In contrast to any of the previously described isoforms of NM II (II-A, II-B0, II-B1, II-C0 and II-C1) or to smooth muscle myosin, the actin-activated MgATPase activity of HMM II-B2 is not significantly increased from a low, basal level by phosphorylation of the 20 kDa myosin light chain (MLC-20). Moreover, although HMM II-B2 can bind to actin in the absence of ATP and is released in its presence, it cannot propel actin in the sliding actin filament assay following MLC-20 phosphorylation. Unlike HMM II-B2, the actin-activated MgATPase activity of a chimeric HMM with the 21-amino acid II-B2 sequence inserted into the homologous location in the heavy chain of HMM II-C is increased following MLC-20 phosphorylation. This indicates that the effect of the II-B2 insert is myosin heavy chain specific.
Published by Elsevier Inc.

Keywords: Nonmuscle myosin II-B; Alternative splicing; Loop 2 insert; Chimeric myosin

Setsuro Ebashi had a major influence on the field of muscle biochemistry and particularly on the regulation of skeletal and cardiac muscle. He made numerous original and important scientific contributions to the field over his entire professional lifetime. He was also distinguished for his modest disposition, his wonderful sense of humor and the kindness he readily bestowed on new and younger scientists entering the field of contractile proteins. Many of us were among those who were fortunate to benefit from his generosity of spirit and kind demeanor in Japan, the U.S.A. and at international meetings. The following article is an original contribution in an area of research he would have appreciated. It deals with an unusual isoform of nonmuscle myosin II (NM II) that is apparently not regulated by phosphorylation of the myosin light chain (MLC-20). It is dedicated to the memory of this outstanding and humane scientist with deep affection.

NM II is a hexamer composed of two heavy chains (230 kDa) and two pairs of light chains (MLC, 20 and 17 kDa). It is present in all eukaryotic cells where it plays a role in cytokinesis, cell motility, cell adhesion, and cell

Abbreviations: aa, amino acid; NMHC, nonmuscle myosin heavy chain; HMM, heavy meromyosin; MHC, myosin heavy chain; MLC, myosin light chain; MLCK, myosin light chain kinase; IVM, *in vitro* motility.

* Corresponding author. Fax: +1 301 402 1542.
E-mail address: AdelsteR@NHLBI.NIH.GOV (R.S. Adelstein).

0006-291X/$ - see front matter Published by Elsevier Inc.
doi:10.1016/j.bbrc.2007.11.108

morphology [1–6]. To date, all mammals studied appear to contain at least three different isoforms of the nonmuscle myosin heavy chain (NMHC) II. The genes encoding the NMHCs in humans are referred to as *MYH9, MYH10,* and *MYH14* and their protein products are called NMHC II-A, II-B and II-C.

Two of the three NMHCs, NMHC II-B and II-C, have been shown to undergo alternative splicing of pre-mRNA in which an exon encoding either 10- (II-B) or 8- (II-C) amino acids (aa) is inserted into the 25–50 kDa domain boundary (loop 1) near the ATP-binding region of the NMHC [7,8]. An alternative exon encoding 7-aa is inserted into the smooth muscle MHC at this same locus [9,10]. We proposed calling this inserted isoform of NMHC II-B, II-B1 and of II-C, II-C1. The noninserted isoform is designated as NMHC II-B0 or II-C0 (Fig. 1; Ref. [11]). In addition, a second exon encoding 21-aa in NMHC II-B has been shown to be inserted into the 50–20 kDa domain boundary (loop 2) within the actin-binding region and we refer to the insert as II-B2 (Fig. 1; Ref. [7]). Recently, we found that 33-aa and 41-aa were inserted into loop 2 of NMHC II-C in humans and mice, respectively (Siddhartha S. Jana, S.K., R.S.A., unpublished data). Previous work had demonstrated that the NMHC II-B2 inserted isoform is predominantly expressed in mouse cerebellum, especially in cerebellar Purkinje cells, during postnatal development of the brain [12,13]. Baculovirus-expressed heavy meromyosins (HMMs) containing the B1 or C1 insert of NMHC II-B and II-C, respectively, showed an increase in the actin-activated MgATPase activity and *in vitro* motility compared to the noninserted isoform [11,14]. The smooth muscle HMM containing an insert of 7-aa in loop 1 also showed a higher velocity of movement of actin filaments *in vitro* and a higher actin-activated MgATPase activity than the noninserted smooth muscle myosin isoform [9].

The importance of loop 2 for myosin function was first suggested by proteolytic cleavage studies [15–18]. The actin-activated MgATPase activity was decreased by proteolytic cleavage in the loop 2 region [15,17]. Thus, cleavage of loop 2 was inhibited in the presence of F-actin [15,16] and reduced the affinity of myosin for F-actin [17]. The importance of loop 2 was also demonstrated in a molecular genetic study showing that the substitution of loop 2 of *Dictyostelium* myosin with loops from other myosins caused a change in the actin-activated MgATPase to values correlating with the activity of the donor myosins [19]. A further detailed study by Murphy and Spudich [20] showed that the V_{max} of the actin-activated MgATPase activity and the affinity of *Dictyostelium* myosin for actin are both affected by substitutions of the loop 2 sequence. Takahashi et al. [21] demonstrated that the insertion of the human II-B2 sequence into the *Dictyostelium* MHC reduced the motor activity of *Dictyostelium* myosin, with reduction of both the maximal actin-activated MgATPase activity and a decrease in the affinity for actin. *In vivo* studies with genetically ablated NMHC II-B2 mice demonstrated impaired motor coordination and misplaced Purkinje cells in the cerebellar molecular layer [13]. However, there has been no *in vitro* characterization of native human NM II-B2 containing the 21-aa insert in loop 2 to date.

In this paper, we focus on the differences in the properties of the noninserted isoform HMM II-B0, and the 21-aa inserted isoform HMM II-B2. We studied the dimeric N-terminal fragment of NM II-B (aa 1–1045), which contains both the actin- and ATP-binding regions and is soluble at relatively low ionic strength, thereby permitting detailed kinetic studies. We used the baculovirus system to express the alternatively spliced isoforms along with MLC-20 and MLC-17. We then characterized each isoform with respect to its actin-activated MgATPase activity and ability to propel actin filaments in the *in vitro* motility assay. We also

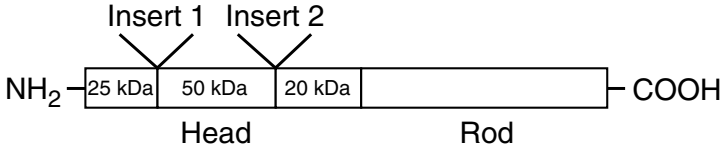

NMHC	Species	Insert Sequence
II-B1	Human	**QESPKPVKHQ**
	Mouse	**QESPKPVKPQ**
II-C1	Human	**ASVSTVSY**
	Mouse	**ASVSTMSY**
II-B2	Human	*ELWKD***EIQNIQRASFYDSVSGLHEPP***VDRIVGLDQVTGMTETAFGSAYKTKKGMFR*
	Mouse	**EIQTIQRASFYDSVSGLHEPP**
II-C0	Mouse	*EIWKD* *VEGIVGLEQVSSLGDGPPGG--RPRRGMFR*

Fig. 1. Diagram of the location of inserted sequences in the NMHC. The diagram of the NMHC molecule shows the location of insert 1 (near the ATP-binding region) and insert 2 (near the acting-binding region). The 25–50 kDa and the 50–20 kDa boundaries designate proteolytic sensitive regions where loop 1 and loop 2 are located. The amino acid sequences of insert 1 and insert 2 are shown in bold. The sequence of amino acids that constitute loop 2 and flank the II-B2 insert are shown in italics. The chimeric HMM II-C0B2 was generated by inserting the human 21-aa sequence shown in bold into the flanking mouse sequence of II-C0 shown on the bottom line. Note the conservation of the loop 2 sequence for NMHC II-B and II-C.

investigated the enzymatic activity of a chimeric HMM with a backbone of HMM II-C containing the NM II-B2 insert, as well as the cellular function of full-length NMHC II-B2 tagged with GFP in COS-7 cells.

Materials and methods

Construction of baculovirus expression vectors. Recombinant HMM-like proteins of human NMHC II-B and mouse NMHC II-C were expressed in the baculovirus/Sf9 system. Briefly, the cDNA (nucleotides 1–3135) for human NMHC II-B (Accession No. M69181 with a change in amino acid Cys 800 to Tyr, which is the more commonly occurring amino acid) and the cDNA (nt 1–4071) for mouse NMHC II-C (Accession No. AY205605) were truncated at amino acid 1045 and 1357, respectively, to create an HMM fragment. Nucleotides encoding a FLAG epitope (DYKDDDDK) followed by a stop signal were appended to aid in purification. To generate a clone of the 21-aa inserted isoform in HMM II-B and HMM II-C, we introduced the 63 nt cassette encoding the II-B2 insert into HMM II-B0 just after nt 1863 and II-C0 just after nt 1908 by recombinant PCR. All HMM constructs were subcloned into the baculovirus transfer vector pFastBac1 (Invitrogen, Carlsbad, CA). Constructs were confirmed by nucleotide sequencing.

Eukaryotic expression plasmid and siRNA oligonucleotides. The Tet-on/off promoter in the expression plasmid containing the GFP-tagged, full-length NMHC II-B [3] was replaced by the cytomegalovirus promoter from the enhanced GFP-N3 vector (Clontech, Palo Alto, CA). NMHC II-B siRNA duplexes (AAGGAUCGCUACUAUUCAGGA) were chemically synthesized by Dharmacon (Lafayette, CO). Control siRNA non-specific duplex (GCGCGCUUUGUAGGAUUCG) was purchased from Dharmacon.

Cell culture and transfection. COS-7 cells were obtained from ATCC (Manassas, VA) and were cultured in Dulbecco's modified Eagle's medium supplemented with 10% heat-inactivated fetal bovine serum. Transient transfections with siRNA and plasmids were carried out using Nucleofector kits according to the manufacturer's instructions (Amaxa, Cologne, Germany) as previously described [3]. The transfection efficiency was about 35% for GFP-tagged NMHC II-B and 95% for NMHC II-B siRNA.

Preparation and purification of HMM proteins. The recombinant HMMs of noninserted and inserted isoforms of NMHC II-B and II-C were expressed in the baculovirus/Sf9 system along with the appropriate light chains [14] and purified according to Wang et al. [22]. Each heavy chain virus was co-infected along with a virus containing both light chains into Sf9 cells at a multiplicity of infection of 10. The infected cells were harvested by sedimentation after 72 h of growth and stored at −80 °C. Western blot analyses of the Sf9 cell pellets demonstrated that significant amounts of the protein were expressed. The partially thawed pellet was extracted with 0.5 M NaCl, 10 mM MOPS (pH 7.3), 10 mM $MgCl_2$, 1 mM EGTA, 3 mM NaN_3, 2 mM ATP, 0.1 mM phenylmethylsulfonylfluoride (PMSF), 0.1 mM dithiothreitol, 5 μg/ml leupeptin, and proteinase inhibitor cocktail (chymostatin, pepstatin A, Tos-Lys-CMK-HCl, and L-1-tosylamide-2-phenyl-ethylchloromethyl-ketone) following homogenization in a ground glass homogenizer and purified by FLAG affinity chromatography. The material eluted from the FLAG column (Sigma, St. Louis, MO) was concentrated using a Q Sepharose column (Amersham, Piscataway, NJ). The protein concentration was determined by Bradford assay using smooth muscle HMM as a standard.

ATPase assays. Actin-activated MgATPase activities were measured by an NADH-linked assay as described by Wang et al. [23] at 25 °C in a buffer containing 10 mM MOPS (pH 7.0), 2 mM $MgCl_2$, 0.1 mM EGTA, 1 mM ATP, 0.2 mM $CaCl_2$, 1 μM calmodulin, 10 μg/ml MLCK, 40 U/ml lactate dehydrogenase, 200 U/ml pyruvate kinase, 1 mM phosphoenolpyruvate, and 0.2 mM NADH plus various concentrations of actin. Actin filaments were stabilized by a 1.5-fold molar excess of phalloidin (Calbiochem, San Diego, CA). Data were corrected for the background ATPase activity of actin. Fitting of experimental datasets to mathematical functions was done using OriginLab 7.0 (Microcal Corp., Northampton, MA). Reported means and standard deviations are those of two to four separate experiments as noted in the Results. The K^+-EDTA ATPase activity was measured in 0.5 M KCl, 2 mM EDTA, 20 mM MOPS (pH 7.2), and 1 mM ATP including [γ-^{32}P] ATP (Perkin-Elmer, Waltham, MA) at 25 °C.

In vitro motility assays (IVMs). Assays were performed at 30 °C in a buffer comprising 50 mM KCl, 20 mM MOPS (pH 7.4), 5 mM $MgCl_2$, 0.1 mM EGTA, 1 mM ATP, 50 mM DTT, 0.2 μM tropomyosin, 0.7% methylcellulose, 2.5 mg/ml glucose, 0.1 mg/ml glucose oxidase, and 2 μg/ml catalase. Each HMM protein was introduced at a protein concentration of 0.2 mg/ml into a flow chamber with a nitrocellulose-coated coverslip. The surface was subsequently blocked by 1 mg/ml BSA, and then incubated for 1 min at room temperature in a solution containing 5 μM unlabeled F-actin, 1 mM ATP, 0.2 mM $CaCl_2$, 1 μM calmodulin, and 4 μg/ml MLCK. After washout, 20 nM F-actin labeled with rhodamine–phalloidin (Molecular Probes, Carlsbad, CA) and the above assay buffer were applied to the flow chamber. The sliding speed of actin filaments over the myosin-coated surface was analyzed using the CellTrak system (Motion Analysis, Santa Rosa, CA) as described earlier [14]. Reported means and standard deviations are those of three separate experiments.

Acto-HMM II-B cosedimentation. Each of the HMM proteins (10 μM) was incubated at 25 °C for 15 min in the absence or presence of 50 μM actin with or without 5 mM ATP containing 1 μM calmodulin, 200 μM $CaCl_2$, 200 U/ml pyruvate kinase, 1 mM phosoenolpyruvate, and 5 μg/ml MLCK. The 100 μl samples were ultracentrifuged at 100,000 rpm in a Beckman TLA-100 rotor for 15 min at 4 °C. The resulting supernatant and pellets were analyzed by SDS 4–20% PAGE (Invitrogen).

Phosphorylation of HMM II-B0 and II-B2. The following kinases were used in an effort to phosphorylate the B2 insert of HMM II-B2: cdc2 kinase (NEB, Ipswich, MA), cdk5 kinase, calmodulin-dependent protein kinase II (NEB), MAP kinase (NEB), casein kinase II (Upstate, Bedford, MA), PDK1 kinase (Upstate), Src kinase (Invitrogen), and cAMP-dependent kinase (NEB) at 30 °C for 10 min according to the manufacturer's instructions. We added 5 ng/μl of each kinase and 0.1 mM ATP including [γ-^{32}P] ATP to each reaction as described previously [14,24]. The reaction was terminated by addition of Laemmli SDS loading buffer and boiled for 5 min. Samples were subjected to electrophoresis in SDS 4–20% polyacrylamide gels. To measure the stoichiometry of phosphate incorporation into the NMHC of HMM II-B0 and II-B2, SDS–PAGE was performed after Src kinase incubation and the Coomassie Blue-stained HMM heavy chain was cut out. ^{32}P incorporated into HMM II-B0 or II-B2 was quantitatively measured by liquid scintillation counting (Beckman, Fullerton, CA). To determine the extent of phosphorylation of MLC-20 by MLCK, HMM II-B0 and II-B2 were phosphorylated in 20 mM KCl, 4 mM $MgCl_2$, 0.2 mM $CaCl_2$, 10 mM MOPS (pH 7.2), 0.1 mM EGTA, 1 μM calmodulin, 0.5 μg/ml MLCK, and 0.2 mM ATP including [γ-^{32}P] ATP at 25 °C for 1, 2, 4, 6, 8, 10, 15, 20, and 30 min. After incubation for the indicated time, each reaction mix was spotted on a filter paper (Whatman, Florham Park, NJ) and washed with 10% TCA and 2% sodium pyrophosphate. The extent of ^{32}P-phosphorylated incorporation into MLC-20 in HMM II-B0 and II-B2 was determined by liquid scintillation counting.

For the actin-activated MgATPase activity assay, HMM II-B0 and II-B2 were phosphorylated by Src kinase, eluted from a Sepharose G-50 column (Amersham), and assayed for activity. In each case, the protein concentration was determined by the Bradford assay.

Immunoblot analysis. HMM subunits were separated by SDS 6%–PAGE (Invitrogen) and transferred to Immobilon-P membranes (Millipore, Bedford, MA). After blocking in phosphate-buffered saline (PBS) containing 5% skim milk and 0.05% Tween 20, the blot was incubated with the monoclonal antibody against phosphotyrosine (Upstate). Horseradish peroxidase-conjugated anti-mouse IgGs were used as secondary antibodies. The blot was visualized by Supersignal West Dura Reagent (Pierce, Rockford, IL).

Immunofluorescence microscopy. Cells grown on 2 well chamber slides were fixed with 4% paraformaldehyde and permeabilized with 0.5% Triton X-100 for 15 min. For antibody staining, the samples were blocked with 10% normal goat serum in 1% bovine serum albumin (BSA) in PBS for 30 min and incubated with NMHC II-B antibody at 4 °C overnight. The

second antibody, Alexa 594-conjugated goat anti-rabbit IgG, was incubated for 1 h at room temperature. The slides were mounted using a Vectashield kit (Vector Laboratories, Burlingame, CA) with DAPI (4′,6′-diamidino-2 phenylindole). The images were collected using a Leica SP confocal microscope (Deerfield, IL).

Results

Enzymatic and motile activity of HMM II-B0 and HMM II-B2

HMM II-B2 has a 21-aa insert in loop 2 starting after residue 621 in human NMHC II-B (see Fig. 1). HMM II-B0 and II-B2 proteins were purified in mg quantities from 1×10^9 cells following baculovirus expression and each HMM heavy chain bound the co-expressed MLC-20 and MLC-17 in an approximate 1:1:1 ratio. Fig. 2A is a Coomassie Blue-stained SDS–polyacrylamide gel showing each of the purified HMMs following concentration using a Q Sepharose column. The enzymatic activity was initially assessed by measuring the MgATPase activities of the two HMMs in the absence of actin, before as well as after phosphorylation of MLC-20 by MLCK. The basal activity in the absence of actin and MLC-20 phosphorylation was very low ($<0.008\ s^{-1}$) for each of the HMM II-B proteins.

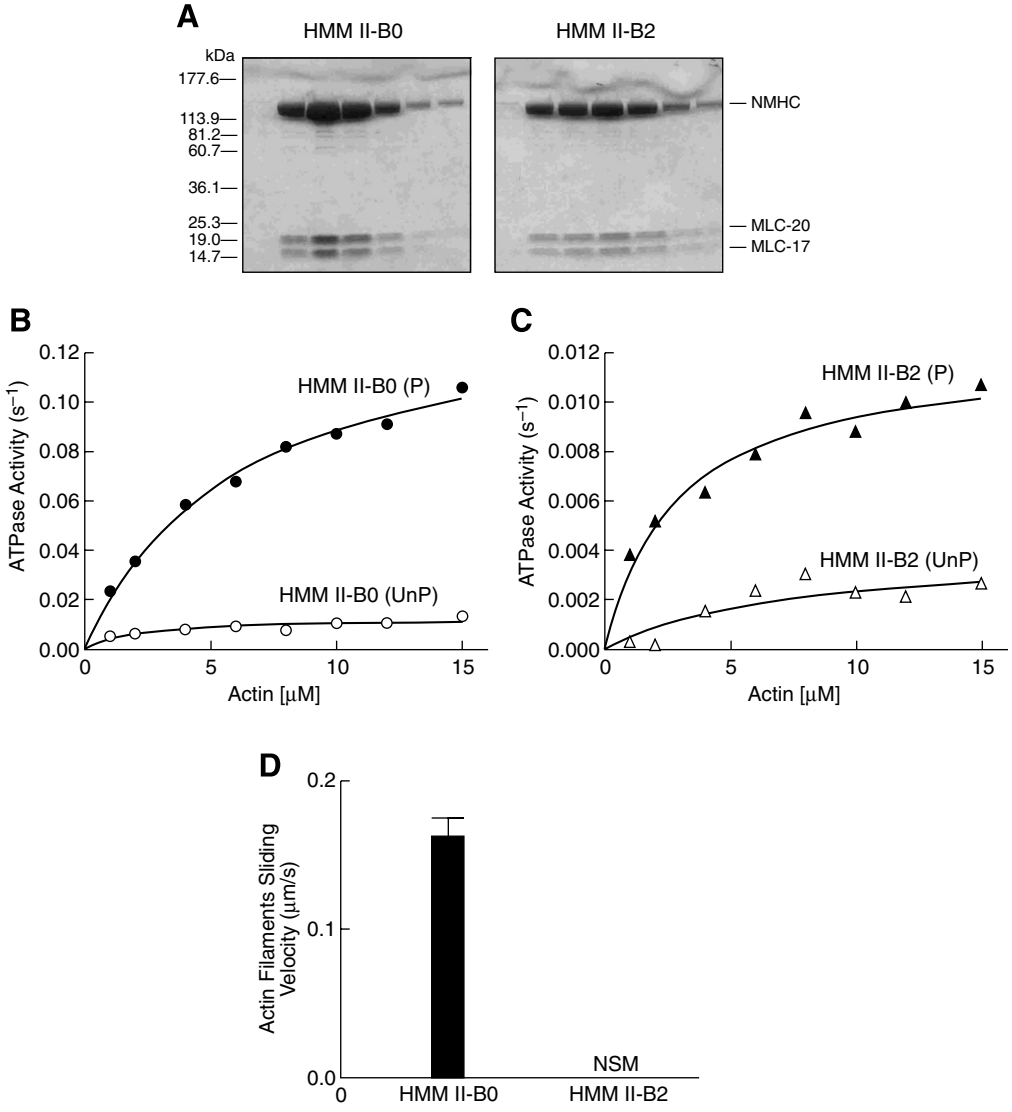

Fig. 2. Purification and activity of HMM II-B0 and II-B2 protein. (A) Coomassie Blue-stained SDS–polyacrylamide gels of column fractions of the concentrated HMM II-B0 and II-B2 eluted from a Q Sepharose column. (B) Actin-activated MgATPase activity of HMM II-B0 was measured before (open circles) and after (closed circles) phosphorylation by MLCK at 25 °C. (C) Actin-activated MgATPase activity of HMM II-B2 before (open triangles) and after (closed triangles) phosphorylation by MLCK. The MgATPase activity of HMM in the absence of actin was subtracted from each data point. Datasets were fitted to a hyperbolic equation (solid lines) to determine the kinetic constants, V_{max} and K_{ATPase} (see Table 1). The data shown are from a single preparation of each HMM. A total of four different preparations were used to prepare Table 1. Note the different scales of ATPase activity (s^{-1}) for (B,C). UnP, unphosphorylated; P, phosphorylated. (D) *In vitro* motility rate for actin filaments using HMM II-B0 or II-B2. Each HMM II-B protein was introduced at a concentration of 0.2 mg/ml into the flow chamber. The sliding velocity was determined for three preparations each of HMM II-B0 and II-B2. The plot shows mean velocity with the standard deviation. No significant movement (NSM) of actin filaments was seen with the HMM II-B2 preparation. All proteins were phosphorylated with MLCK prior to the IVM assays.

Table 1
Summary of actin-activated MgATPase activity and *in vitro* motility of HMM II-B

HMMs	Basal MgATPase (s^{-1})	Actin-activated MgATPase			IVM (μm/s)	K^+-EDTA ATPase (s^{-1})
		−MLCK	+MLCK			
		V_{max} (s^{-1})	V_{max} (s^{-1})	K_{ATPase} (μM)		
II-B0	<0.008	0.008 ± 0.002	0.15 ± 0.02	5.8 ± 0.6	0.16 ± 0.01	0.2
II-B2	<0.006	0.006 ± 0.003	0.01 ± 0.003	2.8 ± 0.8	NSM	0.2

Actin-activated MgATPase activities were measured at 25 °C as described in Materials and methods. The values for V_{max} and K_{ATPase} are the mean and standard deviation from four different protein preparations. The IVM (*in vitro* motility) are from three preparations and the K^+-EDTA ATPase values are the average of two preparations.
II-B0, noninserted HMM II-B; II-B2, inserted HMM II-B with a 21-aa insert; NSM, no significant movement. Basal MgATPase is without actin, but with MLCK.

To date, all vertebrate smooth muscle and NM IIs require phosphorylation of the MLC-20 for full activation of their actin-activated MgATPase activity. As expected, Fig. 2B shows that the actin-activated MgATPase activity of HMM II-B0 increased following phosphorylation by MLCK. The data for each HMM was fitted to a hyperbolic equation to determine the kinetic constants V_{max} (maximal actin-activated MgATPase activity) and K_{ATPase} (actin concentration at half-maximal activation, see Table 1). Surprisingly, following phosphorylation by MLCK, the V_{max} of HMM II-B2 ($0.01 \pm 0.003\ s^{-1}$) was less than 7% of that of phosphorylated HMM II-B0 ($0.15 \pm 0.02\ s^{-1}$). Its K_{ATPase} was slightly lower than that of HMM II-B0 (2.8 ± 0.8 μM for HMM II-B2 compared to 5.8 ± 0.6 μM for HMM II-B0; Fig. 2C and Table 1). The low MgATPase activity of HMM II-B2 appears to be due to its inability to be activated by MLC-20 phosphorylation. Whereas the actin-activated MgATPase activity of HMM II-B0 increased almost 20-fold following MLC-20 phosphorylation, the activity of HMM II-B2 increased less than 2-fold (0.006–0.01 s^{-1}, see Table 1) following phosphorylation.

An important functional property of myosin is its ability to translocate actin filaments. This can be measured using the *in vitro* motility assay (IVM) with rhodamine–phalloidin-labeled actin. The movement of actin filaments over the myosin-coated surface was detected by fluorescence microscopy and the sliding speed was analyzed using the CellTrak system. Both HMMs were phosphorylated using MLCK prior to assay. As Table 1 shows, HMM II-B0 moved actin filaments with an average velocity of 0.16 μm/s. In contrast, we did not observe any significant movement (<0.01 μm/s) of actin filaments bound to HMM II-B2 coated surfaces (Fig. 2D and Table 1). These results indicate that the insertion of 21-aa into the loop 2 of HMM II-B inhibits the actin-activated MgATPase activity following MLC-20 phosphorylation and causes a loss of unloaded *in vitro* motor activity.

Lack of HMM II-B2 activity is not due to dephosphorylation of MLC-20

Since both the actin-activated MgATPase activity and the IVM of NM IIs require MLC-20 phosphorylation, we measured the phosphorylation level of HMM II-B0 and II-B2, following addition of MLCK. The low MgATPase activity was not the result of MLC-20 becoming dephosphorylated during the course of the ATPase assay, as HMM II-B2 (and II-B0) retained its original level of phosphorylation during the MgATPase time course (Fig. 3A). To determine whether the cause of the low activity of HMM II-B2 was due to protein denaturation, the nonphysiological K^+-EDTA ATPase activity of HMM II-B0 and II-B2 was measured in 0.5 M KCl. Table 1 shows that HMM II-B2 had the same K^+-EDTA ATPase activity ($0.2\ s^{-1}$) as the noninserted HMM II-B0 ($0.2\ s^{-1}$). This result indicates that the protein was able to bind and hydrolyze nucleotides under these conditions and was, therefore, not denatured.

Reversible binding of HMM II-B2 to actin in the presence of ATP

We performed qualitative co-sedimentation assays to examine the ability of HMM II-B0 and II-B2 to bind to F-actin. In the absence of F-actin, HMM II-B0 and B2 were found mostly in the supernatant following sedimentation (Fig. 3B, M), whereas both HMMs co-sedimented with 50 μM actin in the absence of nucleotide (Fig. 3B, AM). Following addition of 5 mM ATP to acto-HMM II-B0 and II-B2, each of the isoforms was released from actin and was found in the supernatants (Fig. 3B, AMT). These results indicate that the ability of HMM II-B to bind to actin is not affected by the insertion of 21-aa residues into loop 2 during steady-state ATP hydrolysis. We also analyzed the actin-activated MgATPase activity at increasing ionic strength for HMM II-B2. While the V_{max} value of HMM II-B2 was mostly independent of solution ionic strength, the actin concentration needed for half-maximal activation (K_{ATPase}) was 4-fold greater with increasing ionic strength (Table 1, K_{ATPase} 2.8 μM, Table 2, K_{ATPase} 12.1 μM; Fig. 3C). This behavior is characteristic of myosins in which the so-called weak actin-binding (ATP or ADP·Pi-bound) myosin states are the predominant steady-state intermediates in the actomyosin MgATPase cycle [25].

Specific phosphorylation of the 21-aa insert in HMM II-B2

We considered the possibility that phosphorylation of the 21-aa insert in HMM II-B2 could play a role in activa-

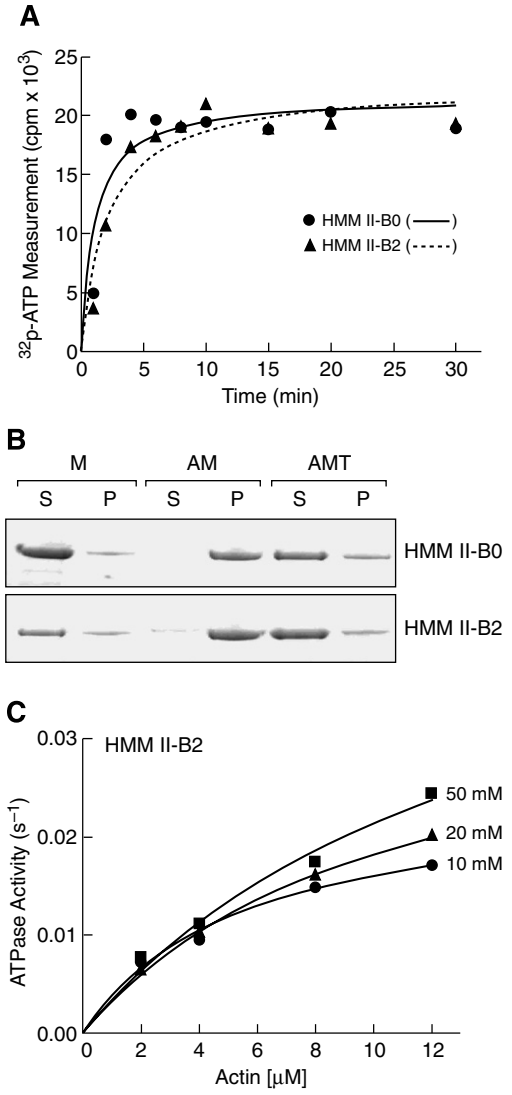

Fig. 3. Phosphorylation, actin-binding and enzymatic activation of HMM II-B2. (A) Phosphorylation of HMM II-B0 and II-B2 by MLCK. HMM II-B was incubated with MLCK using conditions outlined in Materials and methods for the time period shown. Note that both HMM II-B0 and II-B2 were phosphorylated to the same extent and that the level of phosphorylation did not change after 5 min. After incubation for the indicated times, the phosphorylation of HMM II-B0 and II-B2 was determined by liquid scintillation counting. The experiment was repeated twice from two preparations. (B) Acto-HMM II-B0 and II-B2 co-sedimentation. The following samples were analyzed by ultracentrifugation followed by SDS–PAGE: M, 10 μM HMM II-B; AM, 10 μM HMM II-B + 50 μM actin; AMT, 10 μM HMM II-B + 50 μM actin + 5 mM ATP. The HMM II-B0 and II-B2 heavy chain band of the supernatants (S) and pellets (P) are shown. The experiment was repeated twice from two preparations of HMM II-B0 and II-B2. (C) Actin-activated MgATPase activity of HMM II-B2 was measured at 10, 20, and 50 mM KCl concentration after phosphorylation by MLCK. The MgATPase activity of HMM in the absence of actin was subtracted from each data point. Datasets were fitted to the hyperbolic equation (solid lines) to determine the kinetic constants, V_{max} and K_{ATPase}. The values for V_{max} and $K_{ATPases}$ are given in Table 2. The experiment was repeated two times from different preparations.

tion of the actin-activated MgATPase activity because the 21-aa insert (EIQNIQRASFYDSVSGLHEPP) has three serine residues (S) and one tyrosine residue (Y). To determine which kinase might phosphorylate the B2 insert, we incubated HMM II-B2 with cdc2 kinase, cdk5 kinase, calmodulin-dependent protein kinase II, MAP kinase, casein kinase II, PDK1 kinase, Src kinase, or cAMP-dependent kinase. We found that only Src kinase phosphorylated the heavy chain of HMM II-B2, but not II-B0. Fig. 4A and B shows a Coomassie Blue-stained gel and corresponding autoradiogram of HMM II-B0 and II-B2 following phosphorylation by Src kinase and MLCK, respectively. As can be seen from the autoradiogram, only the isoform containing the inserted sequence is phosphorylated on the heavy chain (*). In addition, the MLC-20 of both isoforms is also phosphorylated. To verify which aa was phosphorylated in the B2 insert, HMM II-B0 and II-B2 were incubated with or without Src kinase and then analyzed by immunoblotting with an anti-phosphotyrosine specific antibody. HMM II-B2 heavy chain showed tyrosine-specific phosphorylation after incubation with Src kinase while HMM II-B0 did not (Fig. 4C). Quantification of phosphate incorporation into the single tyrosine residue of the HMM II-B2 inserted region revealed a stoichiometry of 0.2 mol of PO_4/mol of HMM II-B2, assuming that only the tyrosine residue was phosphorylated.

Table 2
Actin-activated steady-state MgATPase parameters of phosphorylated HMM II-B

KCl (mM)	HMM II-B2		HMM II-B0	
	V_{max} (s^{-1})	K_{ATPase} (μM)	V_{max} (s^{-1})	K_{ATPase} (μM)
10	0.02 ± 0.01	5.5 ± 0.3		
20	0.03 ± 0.01	7.2 ± 2.5		
50	0.04 ± 0.01	12.1 ± 2.4	0.15 ± 0.01	6.5 ± 1.3

Actin-activated MgATPase activities were measured at 25 °C in the buffer described in Materials and methods plus KCl. The actin concentration varied from 2 to 12 μM. The values for V_{max} and K_{ATPase} are the mean and standard deviation from two protein preparations.

Enzymatic and motile activity of the Src kinase phosphorylated HMM II-B2

We investigated whether phosphorylation by Src kinase has an effect on HMM II-B2 enzymatic activity. Phosphorylation of HMM II-B2 by Src kinase alone or with MLCK resulted in only a slight increase, if any, in the V_{max} of the actin-activated MgATPase activity (Table 3). The table shows that Src kinase has, at best, a very minor effect on the activity of II-B0 and II-B2. In contrast, MLCK has a major effect on the activity of HMM II-B0, both in the presence and absence of Src kinase. In one experiment, no significant effect of Src kinase phosphorylation was found on the velocity of actin sliding by HMM II-B0 or II-B2. We also repeated the co-sedimentation assays to examine the binding of HMM II-B2 to F-actin before and after phosphorylation by Src kinase. HMM II-B0 and II-B2 showed no difference in their ability to bind to

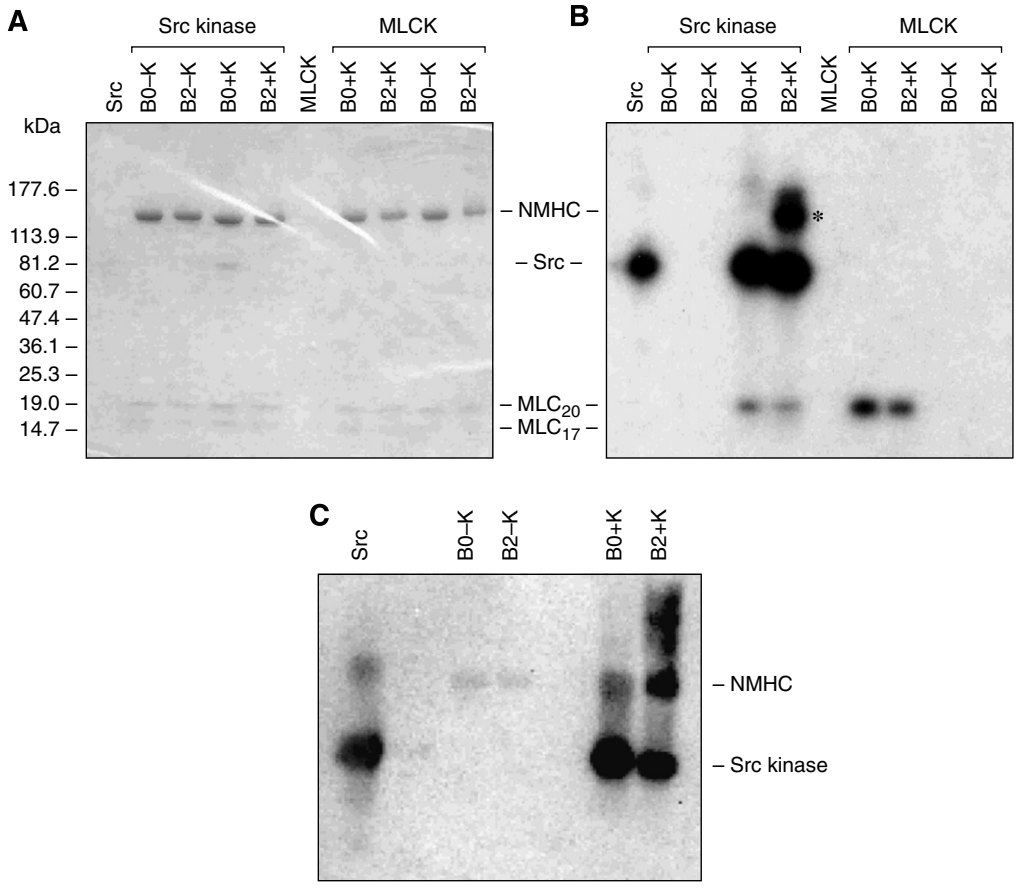

Fig. 4. *In vitro* phosphorylation of HMM II-B2 by Src kinase. HMM II-B0 and II-B2 were incubated with (+K) and without (−K) Src kinase or MLCK. Src kinase alone was incubated without HMM II-B. (A) Coomassie Blue-stained SDS 4–20% polyacrylamide gel of the samples following incubation with the phosphorylation mixture. (B) Autoradiogram of A showing phosphorylation of HMM II-B2 and autophosphorylation of Src kinase. The heavy chain of II-B2 containing the 21-aa insert is phosphorylated (B2+K; Src kinase), but not the II-B0 heavy chain. The asterisk indicates HMM II-B2 heavy chain phosphorylation. The 20 kDa MLC (MLC-20) is also phosphorylated by Src kinase to a small extent. The marker for standard proteins is shown on the *left*. MLCK only phosphorylated MLC-20. Note that the specific activity of the [γ-^{32}P] ATP was approximately 10X greater for the Src kinase reaction mixtures. (C) Immunoblot analysis of phosphorylated HMM II-B2 after incubation with and without Src kinase. The blot was incubated with an anti-phosphotyrosine specific antibody.

Table 3
The effect of phosphorylation by MLCK and Src kinase on the actin-activated MgATPase activity

HMMs	Without Src kinase (V_{max})		With Src kinase (V_{max})	
	−MLCK (s^{-1})	+MLCK (s^{-1})	−MLCK (s^{-1})	+MLCK (s^{-1})
Experiment 1				
II-B0	0.03 ± 0.002	0.17 ± 0.007	0.04 ± 0.005	0.14 ± 0.007
II-B2	0.03 ± 0.005	0.04 ± 0.002	0.07 ± 0.003	0.05 ± 0.003
Experiment 2				
II-B0	0.01 ± 0.01	0.18 ± 0.03	0.03 ± 0.006	0.17 ± 0.02
II-B2	0.01 ± 0.005	0.02 ± 0.003	0.06 ± 0.01	0.04 ± 0.006

Actin-activated MgATPase activities were measured at 25 °C as described in Materials and methods. As a control, we subjected HMM II-B0 to the same assay conditions and measured enzymatic activity before and after addition of Src kinase and MLCK. Each experiment was from different preparations of HMM II-B0 and II-B2.
II-B0, noninserted HMM II-B; II-B2, inserted HMM II-B with a 21-aa insert in loop 2.

actin and be released following addition of ATP before and after Src kinase phosphorylation (data not shown).

Cellular function of NM II-B2 in NMHC II-B siRNA-treated COS-7 cells

To assay the cellular function of full-length NM II-B2, we analyzed cytokinesis in COS-7 cells. Previous work has shown that reducing the amount of NMHC II-B by 85% in COS-7 cells using siRNA resulted in an increase in the percent of multinucleated cells from 9% (control) to 62.4%. This increase in multinucleation could be prevented by transfection with a number of GFP-NMHCs [3]. We, therefore, transfected GFP-tagged full-length NMHC II-B0 or II-B2 into COS-7 cells that had been previously treated with NMHC II-B siRNA for 24 h. Following transfection, the COS-7 cells were cultured for an additional 48 h and then the extent of multinucleation was quantified. Immunofluorescence confirmed the absence of NMHC II-B at 72 h in the siRNA-treated cells that were transfected with GFP alone (Fig. 5A, a–d). The presence of GFP-II-B0 Fig. 5(e–h) and GFP-II-B2 Fig. 5(i–l) as detected by both GFP and an antibody to NMHC II-B is

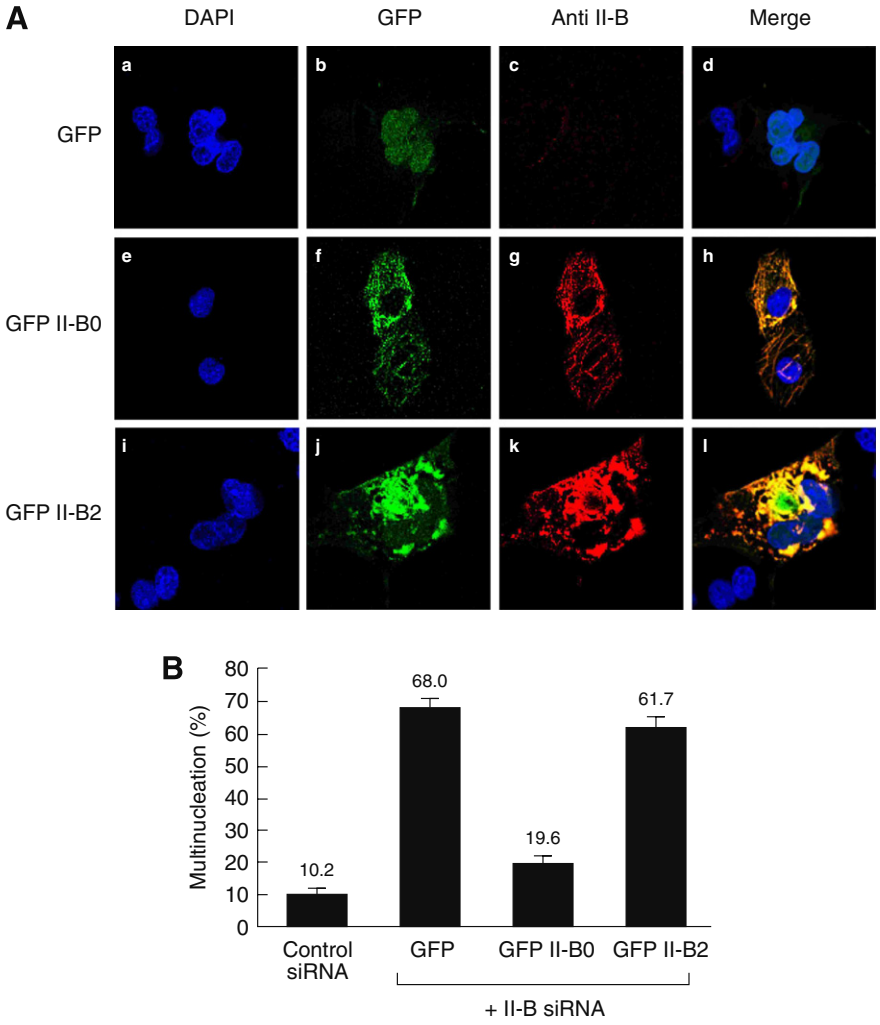

Fig. 5. Failure of full-length NM II-B2 to rescue multinucleation in COS-7 cells. (A) Demonstrates multinucleation in COS-7 cells treated with siRNA to II-B and transfected with GFP alone (a–d; quantified in B). Unlike GFP-II-B0 (e–h), GFP-II-B2 failed to rescue multinucleation (i–l; quantified in B). Yellow indicates cells that were transfected with GFP-labeled constructs (green) and then were stained with anti-II-B antibody (red). Note the aggregation of NMHC II-B2 (see Results). (B) Quantification of multinucleated cells shown in (A). Data are presented as the mean from three independent experiments. In each experiment, at least 100 GFP positive cells were counted.

shown. As quantified in Fig. 5B, control cells transfected with nonspecific siRNA displayed low numbers of multinucleated cells (10.2%). On the other hand, NMHC II-B siRNA-treated cells transfected with GFP alone had an increased number of multinucleated cells (68%). Introducing GFP-NMHC II-B0 into the II-B-depleted COS-7 cells significantly reduced multinucleation (19.6%). In contrast, transfection of GFP-NMHC II-B2 into the II-B siRNA-treated cells failed to rescue multinucleation (61.7%). As can be seen from Fig. 5(i–l), a substantial amount of NM II-B2 is aggregated in the transfected cells and this may have contributed to its inability to rescue multinucleation. It is of note that transfection of GFP-NMHC II-B2 into COS-7 cells that were not previously treated with siRNA to NMHC II-B resulted in GFP-NM II-B2 being incorporated into filaments, suggesting that it is capable of forming co-filaments with NM II-B0 (data not shown).

Enzymatic activity of chimeric HMM II-C0B2, which has the 21-aa B2 insert in loop 2 in HMM II-C0

We were interested in seeing whether the 21-aa II-B2 insert would alter the activity of another HMM isoform, HMM II-C0. Therefore, we cloned chimeric HMM II-C0B2 which has the human 21-aa II-B2 inserted into the homologous loop 2 site in the heavy chain of mouse HMM II-C0 (Fig. 6A and see Fig. 1 for flanking loop 2 aa sequence). Table 4 and Fig. 6B showed that the V_{max} of the actin-activated MgATPase activity of HMM II-C0B2 increased significantly following MLC-20 phosphorylation, similar to HMM II-C0. This is in contrast to HMM II-B2, which had a low V_{max} before and after MLC-20 phosphorylation. Therefore, the effect of the 21-aa II-B2 insert appears to be MHC-specific, since introduction of the II-B2 insert into the HMM II-C0 heavy chain

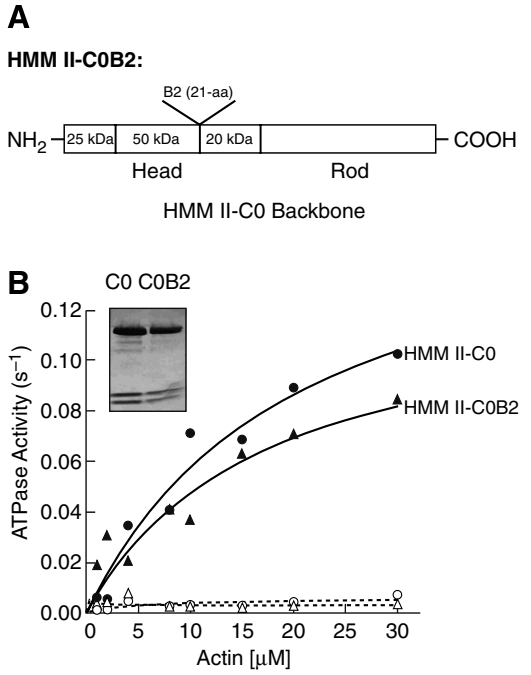

Fig. 6. Actin-activated MgATPase activity of chimeric HMM II-C0B2. (A) The diagram showed the location of the insertion site of the 21-aa, human II-B2 insert into mouse HMM II-C0 (see also Fig. 1). We refer to the chimera as HMM II-C0B2. (B) Actin-activated MgATPase activities of the noninserted HMM II-C0 (circles) and the II-B2 inserted HMM II-C0B2 (triangles) were measured before (open) and after (closed) phosphorylation by MLCK at 25 °C. The insert panel in (B) shows the purified HMM II-C0 and II-C0B2 heavy chains and two light chains stained with Coomassie Blue. The data shown are from a single preparation of each HMM. The experiment was repeated with a second preparation. Datasets were fitted to a hyperbolic equation to determine the kinetic constants, V_{max} and K_{ATPase} (see Table 4).

Table 4
Actin-activated MgATPase activity of chimeric HMM II-C0B2

HMMs	−MLCK	+MLCK	
	V_{max} (s^{-1})	V_{max} (s^{-1})	K_{ATPase} (μM)
Experiment 1			
II-C0	0.04 ± 0.05	0.15 ± 0.03	4.0 ± 1.6
II-C0B2	0.04 ± 0.01	0.13 ± 0.01	6.3 ± 2.1
Experiment 2			
II-C0	0.02 ± 0.01	0.20 ± 0.05	6.0 ± 1.6
II-C0B2	0.01 ± 0.003	0.15 ± 0.04	11.9 ± 1.2

Actin-activated MgATPase activities were measured at 25 °C in the buffer as described in Materials and methods. Each experiment was from a different preparation of HMM II-C0 and II-C0B2.
II-C0, noninserted mouse HMM II-C; II-C0B2, inserted HMM II-C0 with the 21-aa insert of human B2.

backbone did not prevent HMM II-C from being activated by actin following MLC-20 phosphorylation.

Discussion

In this report, we describe the biochemical and cellular characterization of an alternatively spliced isoform of NM II-B. This spliced isoform results from the introduction of 21-aa into the heavy chain of NM II-B in loop 2, at a location that is close to the actin-binding region. A homologous location in NMHC II-C is also used for a larger insert of 33-aa in humans and 41-aa in mice. Of note is that the loop 2 flanking sequence is fairly well conserved between NMHC II-B and II-C (see Fig. 1). We used the soluble HMM derivative of NM II-B so we could carry out kinetic studies of the actin-activated MgATPase activity, that are more difficult with the more insoluble, full-length NM II. Since HMM contains both the actin and ATP binding sites, as well as the locus for the alternatively spliced exon, it appeared to be a reasonable choice, especially since we used noninserted HMM II-B0 for a control.

To our surprise, we found that the V_{max} for the actin-activated MgATPase activity of HMM II-B2 was less than 7% of that for HMM II-B0 following MLC-20 phosphorylation and that HMM II-B2 demonstrated no significant movement in the IVM assay (Table 1). Since this was the first report of a vertebrate NM II that could not be activated following MLC-20 phosphorylation, we were somewhat skeptical of these results. We, therefore, carried out the following experiments: (1) we re-sequenced the HMM II-B2 cDNA encoding the MHC and confirmed that there were no errors. (2) We measured the myosin ATPase activity of HMM II-B2 in 0.5 M KCl in the presence of K^+-EDTA and found that, unlike the actin-activated MgATPase activity, it was similar to that of HMM II-B0. This showed that the ATP binding site was intact and that HMM II-B2 was not denatured. (3) We confirmed that, similar to HMM II-B0, the MLC-20 of HMM II-B2 stayed fully phosphorylated during the actin-activated MgATPase assay. (4) We studied the binding of HMM II-B2 to actin in the presence and absence of ATP and found that, similar to HMM II-B0, it bound and was released from actin in an ATP-dependent manner. (5) We introduced the 21-aa insert into the homologous location in NMHC II-C and found that it did not significantly alter the actin-activated MgATPase activity. This showed that the loss of activity was not simply due to the insert, but required the context of the NM II-B heavy chain.

These experiments lead us to conclude that HMM II-B2 is a unique isoform of NM II that cannot be activated by MLC-20 phosphorylation and may require an alternative mechanism for its activation. Alternatively, its normal function in cells may not require activation of the enzymatic activity. In this regard, it is of interest that when the NMHC II-B2 is specifically ablated in mice, they show abnormalities in cerebellar Purkinje cell localization and these cells had reduced numbers of dendritic spines and branches. These mice also showed impaired motor coordination. Replacement of the NMHC II-B2 with NMHC II-B0 cannot rescue the abnormalities seen in II-B2 insert-ablated mice [13]. These results suggest that the function of NM II-B2 could rely more on the structural (filament-forming) properties of myosin rather than on its enzymatic property, which appears to be lacking. Recently, we have

reported that a mutant form of NM II-B with a decreased actin-activated MgATPase activity can rescue cell adhesion defects in the cells lining the spinal canal [26]. We interpreted these findings as well as the finding that NM II-A could replace II-B in these cells [27] as showing that myosin was playing a structural role in the cells lining the spinal canal and that this function was required to maintain cell adhesion in these cells. Additional experiments will be required to substantiate this possibility in the case of the NM II-B2 insert. Of note however, is that, although the motor activity of HMM II-B2 has been compromised; it is still able to bind to actin and presumably can exert force. Of course, we cannot rule out the possibility that HMM II-B2 can be activated by actin by a yet to be discovered mechanism.

Previous work by others has shown the importance of loop 2 in MLC-20 regulation of HMM activity (for review, see Refs. [28–30]). Rovner et al. [29] replaced loop 2 of smooth muscle HMM with loop 2 from skeletal and cardiac myosin. They found that the chimeric myosins no longer required phosphorylation of MLC-20 for activation and that these myosins had V_{max}s for the actin-activated MgATPase activity and K_ms for actin that correlated with the activities of the loop 2 donor myosins. Furch et al. [31] called attention to the role of charge residues present in loop 2 in modifying the activity of *Dictyostelium* myosin II by introducing lysine residues into loop 2. They found that the introduction of 4–12 extra positive charges resulted in a 2- to 3-fold increase in actin-activated MgATPase activity and a more than 10-fold reduction in K_{app} for actin. It is of note in this respect that the 21-aa insert has a net negative charge. Table 4 shows that the V_{max} of HMM II-C0B2 was only slightly lower than that of the noninserted HMM II-C0. This suggests that the effect of the B2 insert depends on the specificity of myosin heavy chain. In an experiment more directly relevant to the present report, Takahashi et al. [21] introduced loop 2 from II-B0, and separately loop 2 from II-B2, into the *Dictyostelium* myosin II backbone replacing the endogenous loop 2. They found that introducing the II-B0 loop 2 lowered the actin-activated MgATPase activity by one-half compared to the wild-type activity and that introducing the II-B2 loop 2 reduced it by two-thirds. This work differs from that presented here in that both loop 2 from NMHC II-B0 and loop 2 from II-B2 lowered the actin-activated MgATPase activity.

Finally, we speculate that the loss of the actin-activated MgATPase activity in HMM II-B2 compared to II-B0 could be due to the interaction of the 21-aa insert present in II-B2 with the adjacent head on the same HMM, thus inducing the "off state" configuration even when MLC-20 is phosphorylated. This asymmetric intramolecular interaction between the actin-binding region (which includes loop 2) of one head and the converter domain of the second head had been previously reported by others as inducing the "off state" when myosin is dephosphorylated [32–34]. Whether the 21-aa insert in NMHC II-B2 locks the myosin heads in this quiescent state and the physiological relevance of expressing this type of myosin in specialized cells such as the cerebellar Purkinje cells of the brain are questions of continuing interest.

Acknowledgments

We acknowledge the expert technical assistance of Estelle V. Harvey and Antoine Smith. We also acknowledge the expert advice of Mihaly Kovacs. Toshihiko Takenaka generated the original human HMM II-B0 construct. We also thank Catherine S. Magruder for expert editorial assistance and Mary Anne Conti, Mary D. Pato, and Siddhartha S. Jana for reading and improving this manuscript.

References

[1] J.R. Sellers, in: Protein Profile: Myosins, second ed., Oxford University Press, Oxford, 1999.
[2] M.A. Conti, S. Kawamoto, R.S. Adelstein, Nonmuscle myosin II, in: L.M. Coluccio (Ed.), Myosins: a superfamily of molecular motors, Proteins and Cell Regulation, vol. 7, Springer, Dordrecht, The Netherlands, 2008, pp. 223–264.
[3] J. Bao, S.S. Jana, R.S. Adelstein, Vertebrate nonmuscle myosin II isoforms rescue small interfering RNA-induced defects in COS-7 cell cytokinesis, J. Biol. Chem. 280 (2005) 19594–19599.
[4] X. Ma, S. Kawamoto, Y. Hara, R.S. Adelstein, A point mutation in the motor domain of nonmuscle myosin II-B impairs migration of distinct groups of neurons, Mol. Biol. Cell 15 (2004) 2568–2579.
[5] M.A. Conti, S. Even-Ram, C. Liu, K.M. Yamada, R.S. Adelstein, Defects in cell adhesion and the visceral endoderm following ablation of nonmuscle myosin heavy chain II-A in mice, J. Biol. Chem. 279 (2004) 41263–41266.
[6] S. Even-Ram, A.D. Doyle, M.A. Conti, K. Matsumoto, R.S. Adelstein, K.M. Yamada, Myosin IIA regulates cell motility and actomyosin-microtubule crosstalk, Nat. Cell Biol. 9 (2007) 299–309.
[7] M. Takahashi, S. Kawamoto, R.S. Adelstein, Evidence for inserted sequences in the head region of nonmuscle myosin specific to the nervous system, J. Biol. Chem. 267 (1992) 17864–17871.
[8] E. Golomb, X. Ma, S.S. Jana, Y.A. Preston, S. Kawamoto, N.G. Shoham, E. Goldin, M.A. Conti, J.R. Sellers, R.S. Adelstein, Identification and characterization of nonmuscle myosin II-C, a new member of the myosin II family, J. Biol. Chem. 279 (2004) 2800–2808.
[9] C.A. Kelley, M. Takahashi, J.H. Yu, R.S. Adelstein, An insert of seven amino acids confers functional differences between smooth muscle myosins from the intestines and vasculature, J. Biol. Chem. 268 (1993) 12848–12854.
[10] P. Karagiannis, G.J. Babu, M. Periasamy, F.V. Brozovich, The smooth muscle myosin seven amino acid heavy chain insert's kinetic role in the crossbridge cycle for mouse bladder, J. Physiol. 547 (2003) 463–473.
[11] K.Y. Kim, M. Kovacs, S. Kawamoto, J.R. Sellers, R.S. Adelstein, Disease-associated mutations and alternative splicing alter the enzymatic and motile activity of nonmuscle myosins II-B and II-C, J. Biol. Chem. 280 (2005) 22769–22775.
[12] K. Itoh, R.S. Adelstein, Neuronal cell expression of inserted isoforms of vertebrate nonmuscle myosin heavy chain II-B, J. Biol. Chem. 270 (1995) 14533–14540.
[13] X. Ma, S. Kawamoto, J. Uribe, R.S. Adelstein, Function of the neuron-specific alternatively spliced isoforms of nonmuscle myosin II-B during mouse brain development, Mol. Biol. Cell 15 (2006) 2138–2149.
[14] M.D. Pato, J.R. Sellers, Y.A. Preston, E.V. Harvey, R.S. Adelstein, Baculovirus expression of chicken nonmuscle heavy meromyosin II-

B: characterization of alternatively spliced isoforms, J. Biol. Chem. 271 (1996) 2689–2695.
[15] D. Mornet, P. Pantel, E. Audemard, R. Kassab, The limited tryptic cleavage of chymotryptic S-1: an approach to the characterization of the actin site in myosin heads, Biochem. Biophys. Res. Commun. 89 (1979) 925–932.
[16] K. Yamamoto, T. Sekine, Interaction of myosin subfragment-1 with actin: I. Effect of actin binding on the susceptibility of subfragment-1 to trypsin, J. Biochem. (Tokyo) 86 (1979) 1855–1862.
[17] K. Yamamoto, T. Sekine, Interaction of myosin subfragment-1 with actin: III. Effect of cleavage of the subfragment-1 heavy chain on its interaction with actin, J. Biochem. (Tokyo) 86 (1979) 1869–1881.
[18] J. Botts, A. Muhlrad, R. Takashi, M.F. Morales, Effects of tryptic digestion on myosin subfragment-1 and its actin-activated ATPase, Biochemistry 21 (1982) 6903–6905.
[19] T.Q.P. Uyeda, K.M. Ruppel, J.A. Spudich, Enzymatic activities correlate with chimaeric substitutions at the actin-binding face of myosin, Nature 368 (1994) 567–569.
[20] C.T. Murphy, J.A. Spudich, The sequence of the myosin 50–20K loop affects myosin's affinity for actin throughout the actin-myosin ATPase cycle and its maximum ATPase activity, Biochemistry 38 (1999) 3785–3792.
[21] M. Takahashi, K. Takahashi, Y. Hiratsuka, K. Uchida, A. Yamagishi, T.Q.P. Uyeda, M. Yazawa, Functional characterization of vertebrate nonmuscle myosin IIB isoforms using *Dictyostelium* chimeric myosin II, J. Biol. Chem. 276 (2001) 1034–1040.
[22] F. Wang, E.V. Harvey, M.A. Conti, D. Wei, J.R. Sellers, A conserved negatively charged amino acid modulates function in human nonmuscle myosin IIA, Biochemistry 39 (2000) 5555–5560.
[23] F. Wang, M. Kovacs, A. Hu, J. Limouze, E.V. Harvey, J.R. Sellers, Kinetic mechanisms of non-muscle myosin IIB: functional adaptations for tension generation and maintenance, J. Biol. Chem. 278 (2003) 27439–27448.
[24] C.A. Kelly, R.S. Adelstein, The 204-kDa smooth muscle myosin heavy chain is phosphorylated in intact cells by casein kinase II on a serine near the carboxyl terminus, J. Biol. Chem. 265 (1990) 17876–17882.
[25] M. Kovacs, F. Wang, J.R. Sellers, Mechanism of actin of myosin X, a membrane-associated molecular motor, J. Biol. Chem. 280 (2005) 15071–15083.
[26] X. Ma, J. Bao, R.S. Adelstein, Loss of cell adhesion causes hydrocephalus in nonmuscle myosin II-B-ablated and mutated mice, Mol. Biol. Cell 18 (2007) 2305–2312.
[27] J. Bao, X. Ma, C. Liu, R.S. Adelstein, Replacement of nonmuscle myosin II-B with II-A rescues brain but not cardiac defects in mice, J. Biol. Chem. 282 (2007) 22102–22111.
[28] C.T. Murphy, J.A. Spudich, Variable surface loops and myosin activity: accessories to a motor, J. Muscle Res. Cell Motil. 21 (2000) 139–151.
[29] A.S. Rovner, Y. Freyzon, K.M. Trybus, Chimeric substitutions of the actin-binding loop activate dephosphorylated but not phosphorylated smooth muscle heavy meromyosin, J. Biol. Chem. 270 (1995) 30260–30263.
[30] A.S. Rovner, A long weakly charged actin-binding loop is required for phosphorylation-dependent regulation of smooth muscle myosin, J. Biol. Chem. 273 (1998) 27939–27944.
[31] M. Furch, M.A. Geeves, D.J. Manstein, Modulation of actin affinity and actomyosin adenosine triphosphatase by charge changes in the myosin motor domain, Biochemistry 37 (1998) 6317–6326.
[32] T. Wendt, D. Taylor, K.M. Trybus, K. Taylor, Three-dimensional image reconstruction of dephosphorylated smooth muscle heavy meromyosin reveals asymmetry in the interaction between myosin heads and placement of subfragment 2, Proc. Natl. Acad. Sci. USA 98 (2001) 4361–4366.
[33] J. Liu, T. Wendt, D. Taylor, K. Taylor, Refined model of the 10S conformation of smooth muscle myosin by cryo-electron microscopy 3D image reconstruction, J. Mol. Biol. 329 (2003) 963–972.
[34] F. Tama, M. Feig, J. Liu, C.L. Brooks III, K.A. Taylor, The requirement for mechanical coupling between head and S2 domains in smooth muscle myosin ATPase regulation and its implications for dimeric motor function, J. Mol. Biol. 345 (2005) 837–854.